Reaction : ^{10}B(p,α)^{7}Be

The experimental data from BU50, BR51b, JE64, SZ72, RO79, YO91, KN93 and AN93 are used. The thick target yields from RO79 are converted into cross section data using stopping power information [ZI85]. The data from BA55 are in strong disagreement with the other low energy data, and are omitted. The S-factor shows a steep increase with decreasing energy due to the presence of a low energy ($\ell = 0$) resonance at $E_r = (9 \pm 2)$ keV [WI83]. This resonance dominates the S-factor up to an energy of about 400 keV [see also ^{10}B(p,γ)^{11}C]. From the parameters $\sigma_r = (2.07 \pm 0.40) \times 10^{-14}$ μb, $\Gamma_\gamma/\Gamma_{tot} = (2.6 \pm 0.15) \times 10^{-4}$ and $\Gamma_{tot} = 15 \pm 1$ keV [WI83], we obtain $\Gamma_p = (1.0 \pm 0.2) \times 10^{-17}$ keV ($\Gamma_\alpha \simeq \Gamma_{tot}$). For $E < 18.7$ keV, the S-factor is approximated by a Breit-Wigner expression using these parameters. We have studied the influence of the energy error by calculating the reduced width γ^2 corresponding to an energy of 9 keV, and the S-factor curves for 7 and 11 keV and this γ^2. The error of σ_r, $\Gamma_\gamma/\Gamma_{tot}$ and Γ_{tot} is also added. The results show that the uncertainty in the rates is large at temperatures below 0.001, but for $T_9 \geq 0.003$ and in the region of the Breit-Wigner approximation, the error is not larger than 30%. At higher energies, a broad resonant structure dominates the S-factor. The reaction rates are calculated by interpolating linearly the data points. The large differences between the adopted rates and the CA88 ones at low temperatures are due to the contribution of the 10 keV resonance, which is not included in CA88.

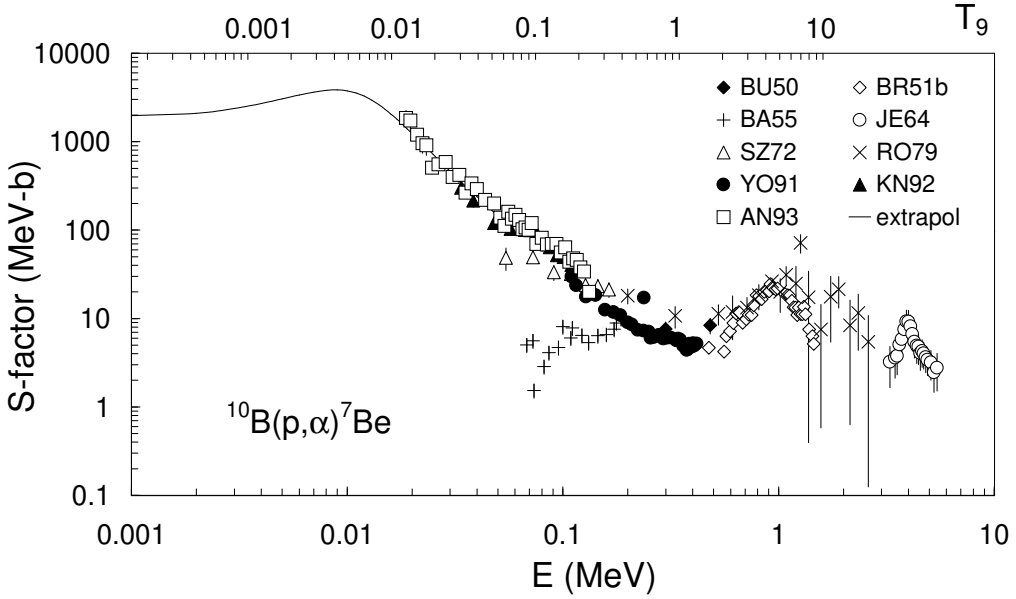

T_9	low	adopt	high	exp	ratio	T_9	low	adopt	high	exp	ratio	T_9	low	adopt	high	exp	ratio
0.003	0.96	1.25	1.53	-21	430	0.06	5.18	5.70	6.23	-1	18	0.7	1.71	1.98	2.24	5	1.2
0.004	1.72	2.23	2.74	-18	450	0.07	1.84	2.03	2.21	0	15	0.8	2.64	3.13	3.61	5	1.1
0.005	3.30	4.29	5.27	-16	430	0.08	5.28	5.79	6.31	0	13	0.9	4.03	4.92	5.82	5	1.1
0.006	1.72	2.23	2.75	-14	400	0.09	1.24	1.36	1.48	1	12	1	5.69	7.15	8.61	5	1.1
0.007	3.86	5.01	6.16	-13	360	0.1	2.52	2.76	3.00	1	10	1.25	1.29	1.71	2.14	6	1.2
0.008	4.85	6.30	7.74	-12	320	0.11	4.88	5.36	5.83	1	9.2	1.5	2.44	3.35	4.26	6	1.1
0.009	4.04	5.24	6.43	-11	280	0.12	8.63	9.48	10.3	1	8.4	1.75	4.22	5.91	7.59	6	1.1
0.01	2.47	3.19	3.91	-10	250	0.13	1.41	1.54	1.68	2	7.7	2	6.54	9.35	12.2	6	1.1
0.011	1.18	1.52	1.86	-9	220	0.14	2.16	2.38	2.60	2	7.0	2.5	1.26	1.87	2.47	7	1.0
0.012	4.70	6.02	7.34	-9	195	0.15	3.23	3.56	3.89	2	6.5	3	2.00	3.06	4.12	7	0.9
0.013	1.59	2.02	2.46	-8	170	0.16	4.55	5.02	5.50	2	5.9	3.5	2.75	4.35	5.96	7	0.9
0.014	4.73	5.98	7.23	-8	155	0.18	8.45	9.37	10.3	2	5.1	4	3.50	5.73	7.95	7	0.9
0.015	1.27	1.59	1.91	-7	140	0.2	1.42	1.57	1.73	3	4.4	5	4.80	8.29	11.8	7	0.9
0.016	3.08	3.84	4.59	-7	120	0.25	3.99	4.44	4.89	3	3.4	6	0.58	1.05	1.51	8	1.1
0.018	1.50	1.83	2.16	-6	100	0.3	8.49	9.44	10.4	3	2.7	7	0.65	1.23	1.80	8	1.2
0.02	5.78	6.94	8.09	-6	83	0.35	1.47	1.64	1.81	4	2.1	8	0.70	1.36	2.01	8	1.4
0.025	8.61	9.97	11.3	-5	58	0.4	2.53	2.81	3.10	4	1.9	9	0.79	1.52	2.25	8	1.7
0.03	6.70	7.60	8.50	-4	44	0.45	3.78	4.22	4.66	4	1.6	10	0.85	1.63	2.42	8	2.0
0.04	1.29	1.43	1.58	-2	29	0.5	5.58	6.23	6.87	4	1.5						
0.05	1.06	1.17	1.29	-1	22	0.6	1.03	1.17	1.30	5	1.3						